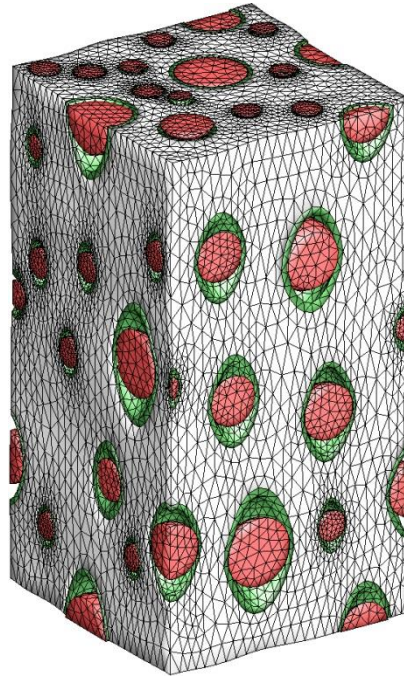


Computational Homogenization of the Debonding of Particle Reinforced Elastomers: Considering Interphases



Daniel Spring

Advisor: Glaucio H. Paulino

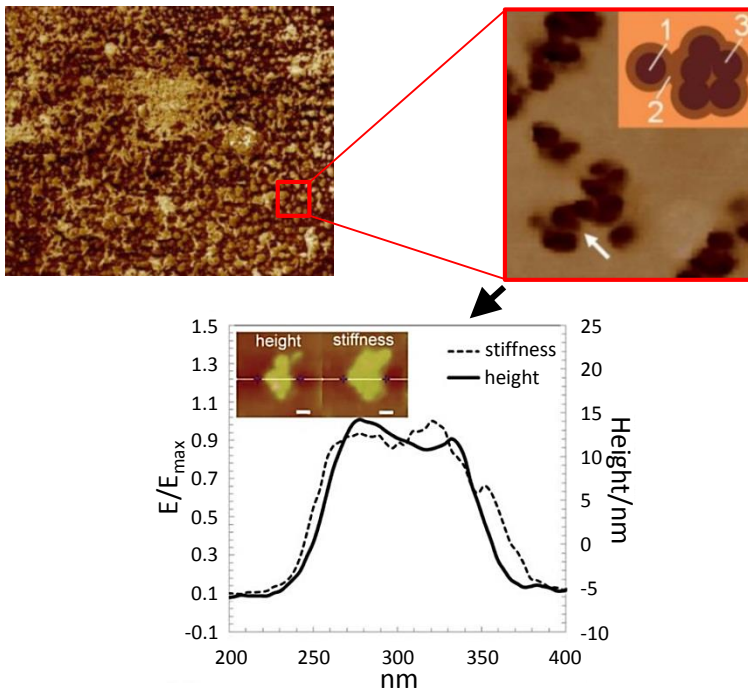
**Department of Civil and Environmental Engineering
University of Illinois at Urbana-Champaign**

October 2nd 2014

Motivation – Presence and Influence of Interphases

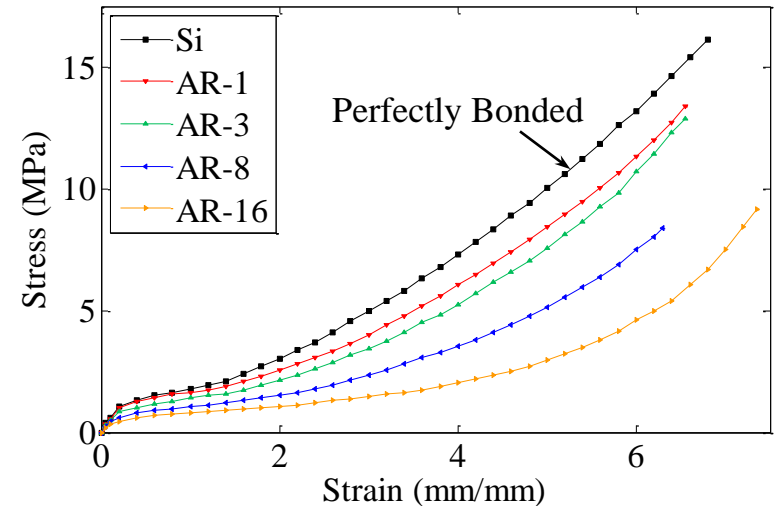
Microscale

When a polymer is reinforced with particles, the polymer chains tend to adsorb onto the surface of the particle:



Macroscale

Ramier investigated the influence of different surface treatments on the macroscopic response of particle reinforced polymers:



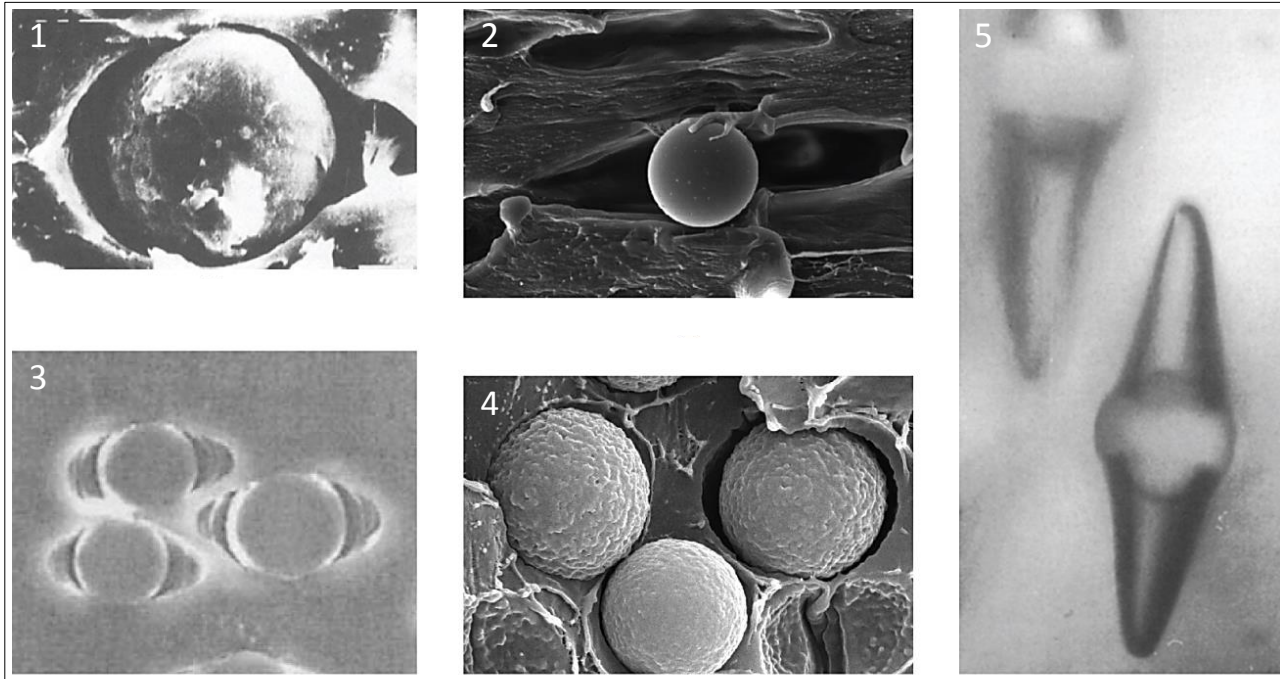
Qu, M., Deng, F., Kalkhoran, S.M., Gouldstone, A., Robisson, A., and Van Vliet, K.J., 2011. Nanoscale visualization and multiscale mechanical implications of bound rubber interphases in rubber-carbon black nanocomposites. *Soft Matter*. Vol. 7, pp. 1066-1077.

Stawhecker, K.E., Hsieh, A.J., Chantawansri, T.L. Kalcioğlu, Z.I. and Van Vliet, K.J., 2013. Influence of microstructure on micro-/nano-mechanical measurements of select model transparent poly(urethane urea) elastomers. *Polymer*. Vol. 54, pp.901-908.

Ramier, J., 2004. Comportement mécanique d'élastomères chargés, influence de l'adhésion charge – polymère, influence de la morphologie. PhD Dissertation, L'Institut National des Sciences Appliquées de Lyon.

Motivation – Interfacial Failure Under Large Deformations

Several experimental investigations have shown the clear localization of failure (debonding) around inclusions, in particle reinforced elastomers, at large strains.



¹Lahiri, J., Paul, A., 1985. Effect of interface on the mechanical behavior of glass bead-filled PVC. *Journal of Materials Science*, Vol. 20, pp. 2253–2259

²Bai S.-L., Chen, J., Huang, Z., Yu, Z., 2000. The role of the interfacial strength in glass bead filled HDPE. *Journal of Materials Science Letters*, Vol. 19, pp. 1587–1589.

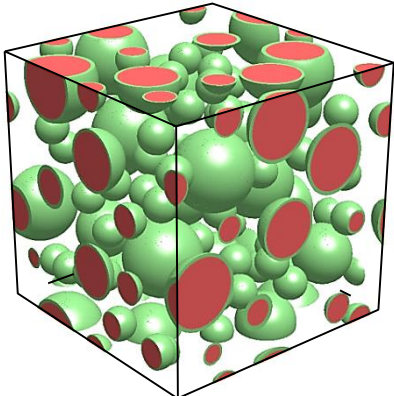
³Thio, Y. S., Argon, A. S., Cohen, R. E., 2004. Role of interfacial adhesion strength on toughening polypropylene with rigid particles. *Polymer*, Vol. 45, pp. 3139–3147.

⁴Renner, K., 2010. Micromechanical deformation process in polymer composites, Ph.D. thesis, Budapest University of Technology and Economics.

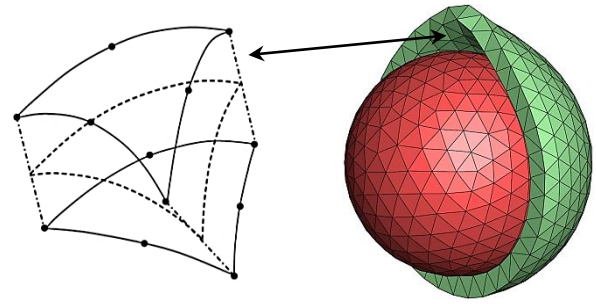
⁵Zhuk, A. V., Knunyants, N. N., Oshmyan, V. G., Topolkaev, V. A., Berlin, A. A., 1993. Debonding microprocesses and interfacial strength in particle-filled polymer materials. *Journal of Materials Science*, Vol. 28, pp. 4595–4606.

Outline

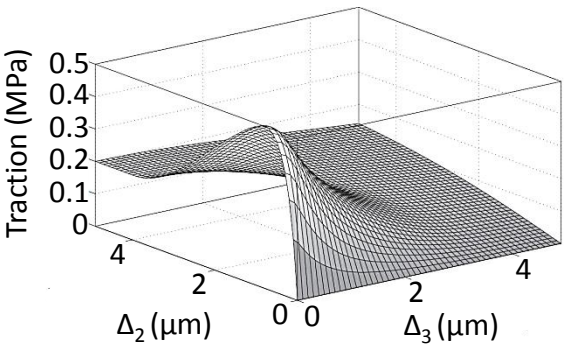
Numerical Model Generation



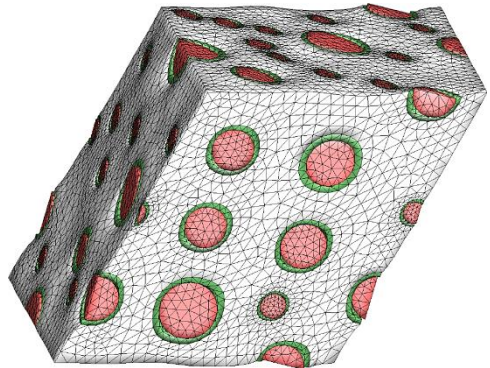
Cohesive Element Formulation



Coupled Cohesive-Friction Model



Large Deformation Results/Discussion

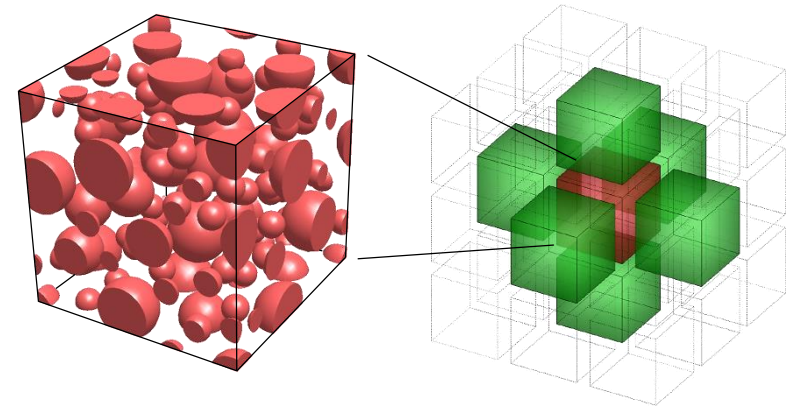


Polydisperse Representative Volume Elements (RVEs)

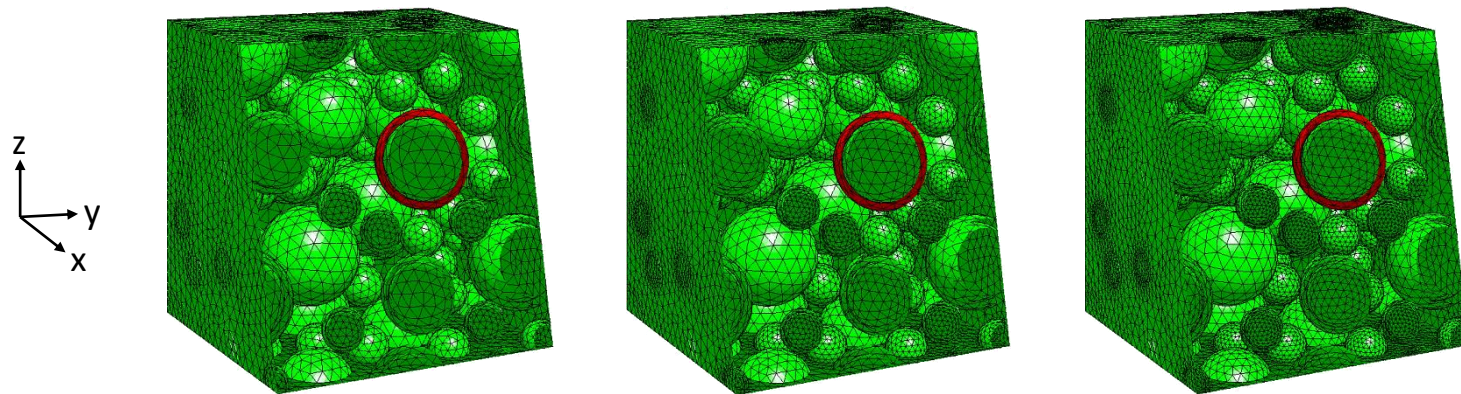
Particles and their associated interphases are placed within the microstructure randomly, using random sequential adsorption¹.

$$10_{\text{large}} + 10_{\text{medium}} + 60_{\text{small}} = 80_{\text{total}}$$

Microstructures are periodic, i.e, one could copy and paste the model in all six directions, and the microstructure would be continuous.



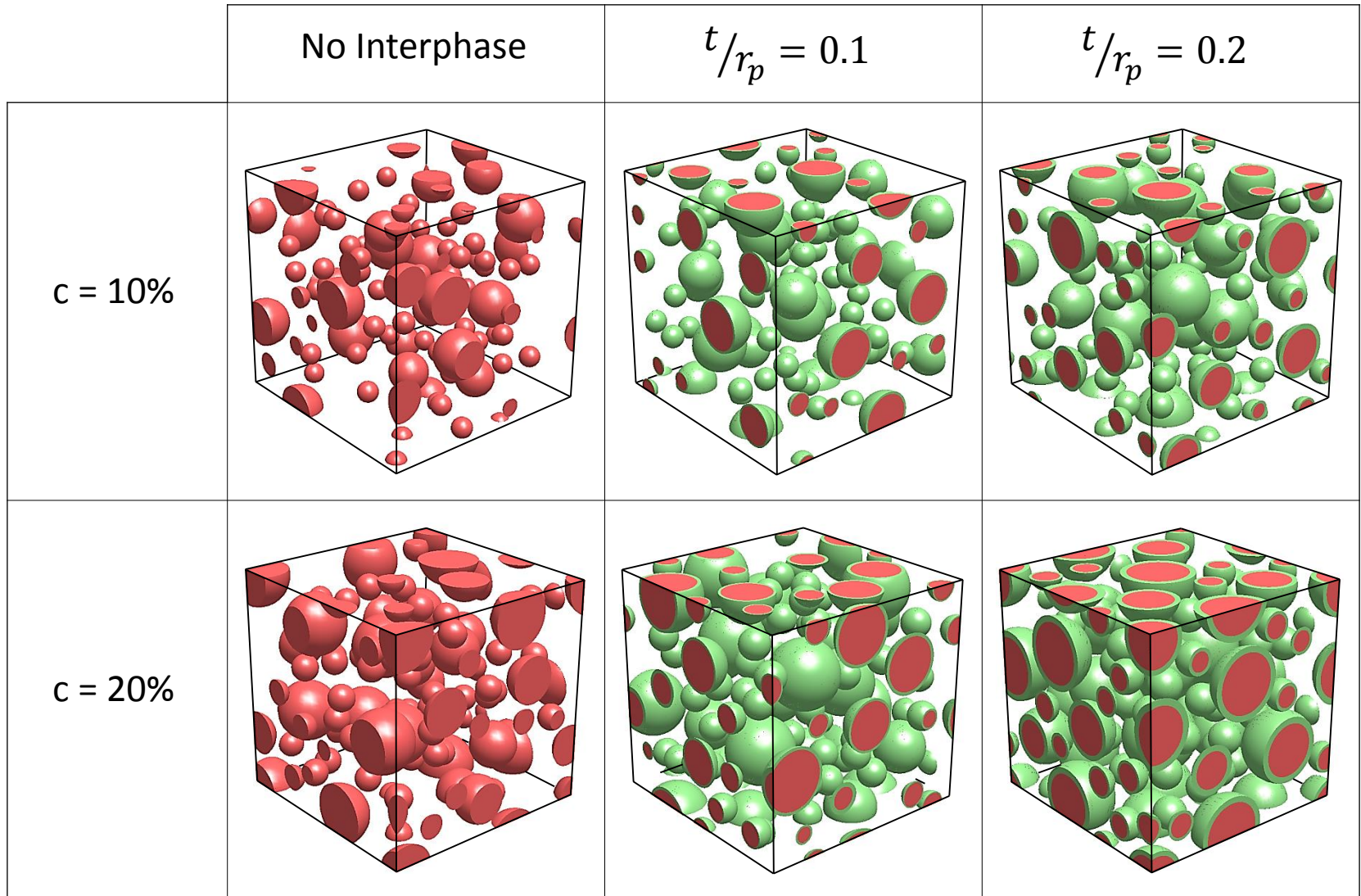
The periodic mesh is generated using the automatic mesh generator Netgen².



¹Feder, J., 1980. Random sequential adsorption. *Journal of Theoretical Biology*, Vol. 87, pp. 237–254.

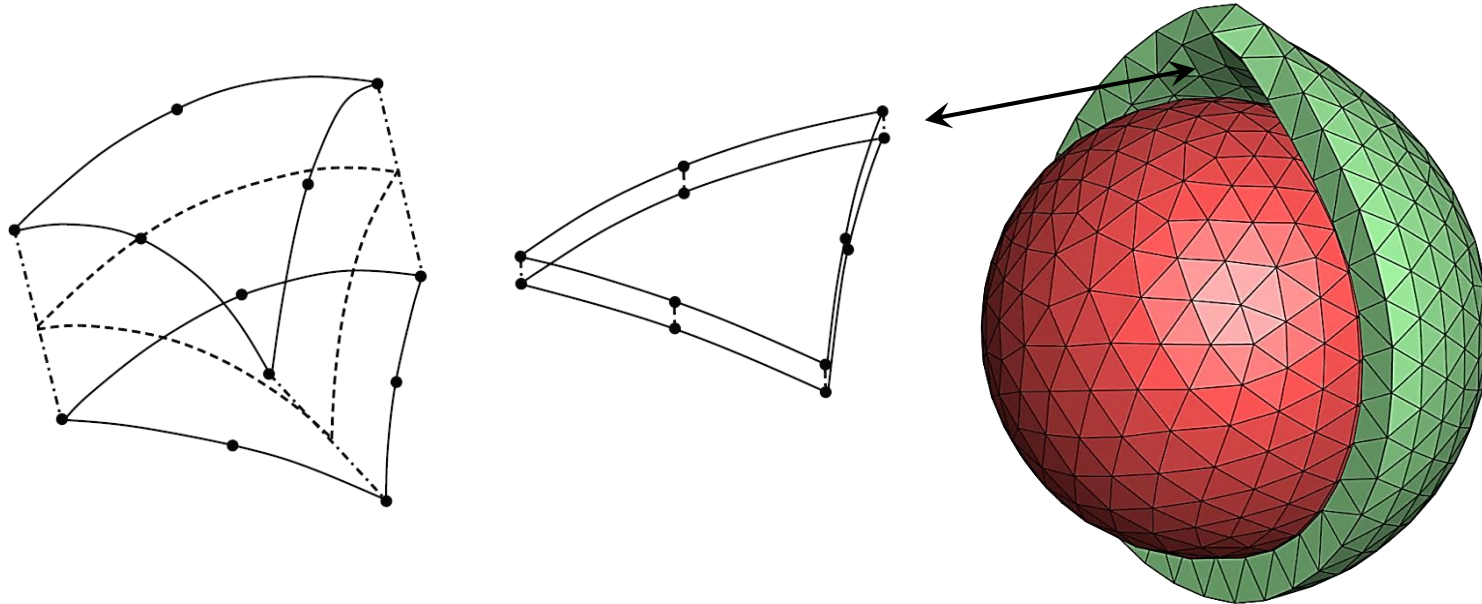
²Schröberl, J., 1997. NETGEN - an advancing front 2D/3D-mesh generator based on abstract rules. *Computing and Visualization in Science*, Vol. 1, pp. 41–52.

Typical Polydisperse Microstructures



Cohesive Elements Account for Interfacial Debonding

The intrinsic cohesive elements are compatible with quadratic tetrahedral bulk elements:



$$[\mathbf{K}]_{\text{coh}} = \int_0^1 \int_0^1 \mathbf{B}^T \mathbf{R}^T \mathbf{D}_{\text{local}} \mathbf{R} \mathbf{B} J d\xi d\eta \quad [\mathbf{F}]_{\text{coh}} = \int_0^1 \int_0^1 \mathbf{B}^T \mathbf{R}^T \mathbf{t}_{\text{local}} J d\xi d\eta$$

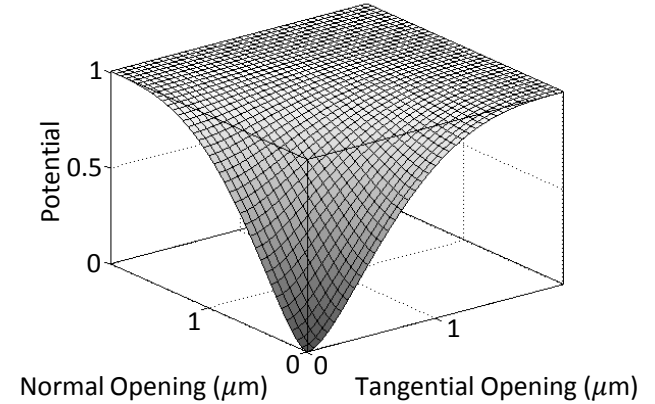
The cohesive elements are implemented as a user defined subroutine in a commercial software package¹.

¹Spring, D. W. and Paulino, G.H., 2014. A growing library of cohesive elements for use in ABAQUS. *Engineering Fracture Mechanics*, Vol. 126, pp. 190-216.

Park-Paulino-Roesler (PPR) Cohesive Model

The cohesive model is defined by a potential:

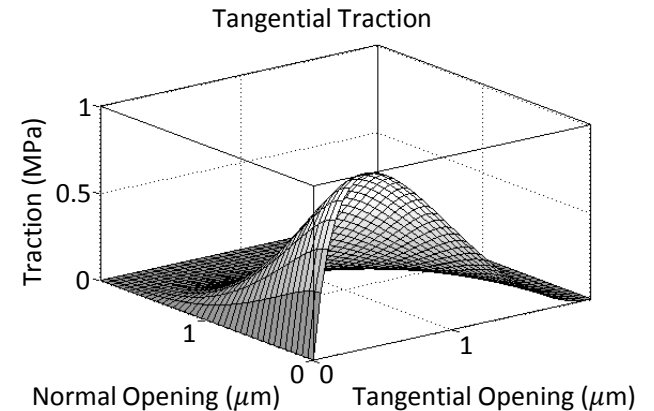
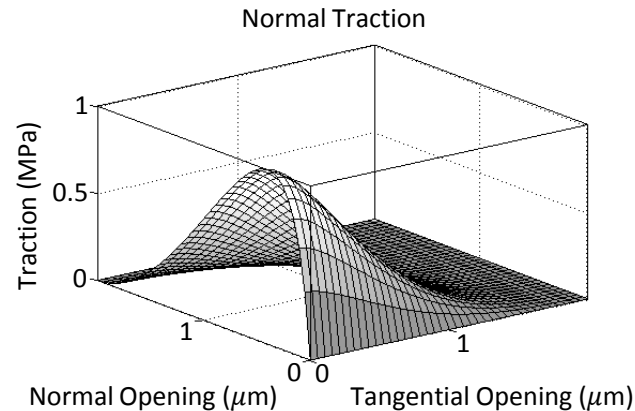
$$\Psi(\Delta_n, \Delta_t) = \min(\phi_n, \phi_t) + \left[\Gamma_n \left(1 - \frac{\Delta_n}{\delta_n} \right)^\alpha \left(\frac{m}{\alpha} + \frac{\Delta_n}{\delta_n} \right)^m + \langle \phi_n - \phi_t \rangle \right] \\ \times \left[\Gamma_t \left(1 - \frac{|\Delta_t|}{\delta_t} \right)^\beta \left(\frac{n}{\beta} + |\Delta_t| \delta_t \right)^n + \langle \phi_t - \phi_n \rangle \right]$$



From the cohesive potential, one can determine the traction-separation relations by taking the respective derivatives

$$T_n(\Delta_n, \Delta_t) = \frac{\partial \Psi}{\partial \Delta_n},$$

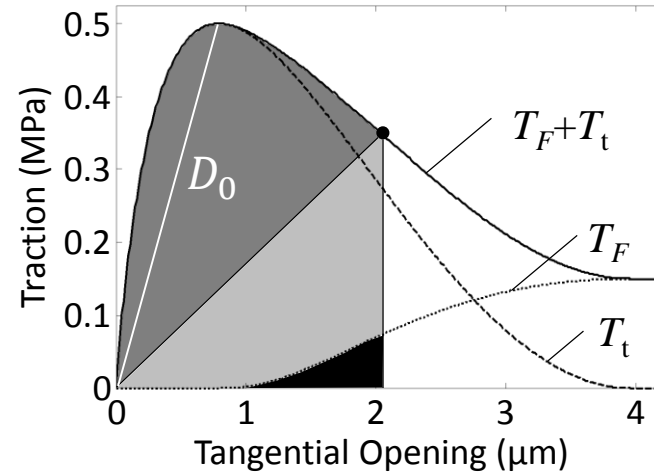
$$T_t(\Delta_n, \Delta_t) = \frac{\partial \Psi}{\partial \Delta_t},$$



Coupled Cohesive-Friction Model

To account for friction at the interface, we developed a new coupled cohesive-friction model. The contribution of friction to the tangential force is described as:

$$\mathbf{T} = \begin{Bmatrix} T_t \frac{\Delta_2}{\Delta_t} + T_F \left(\frac{|\Delta_2|}{\Delta_t} \right) \frac{\dot{\Delta}_2}{|\dot{\Delta}_2|} \\ T_t \frac{\Delta_3}{\Delta_t} + T_F \left(\frac{|\Delta_3|}{\Delta_t} \right) \frac{\dot{\Delta}_3}{|\dot{\Delta}_3|} \end{Bmatrix}$$



The above model is general. However, the newly proposed friction model is designed to be coupled to the PPR cohesive model, and adjusts as the cohesive model adjusts:

$$T_F = \mu \kappa(\Delta_t) |T_n|, \quad \kappa(\Delta_t) = \left(1 - \frac{T_t(0, \Delta_t)}{D_0 \Delta_t} \right)^s \quad \text{if } T_n < 0 \text{ and } \Delta_t > \lambda_t \delta_t$$

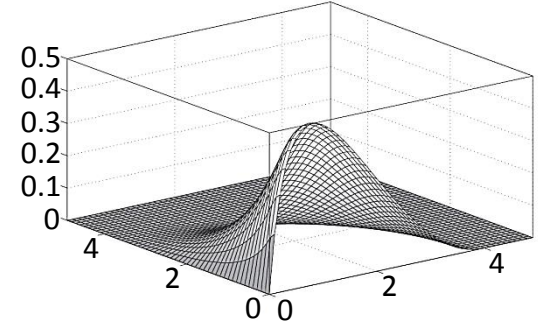
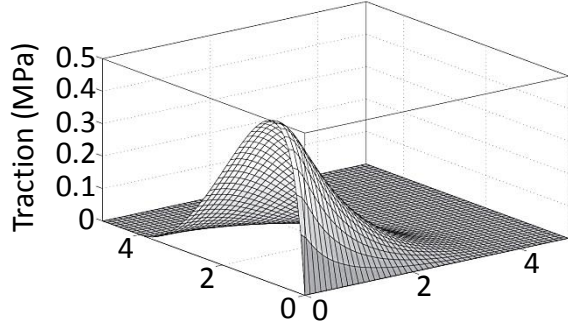
where:

$$D_0 = \frac{\Gamma_t}{\delta_t} \left[n(1 - \lambda_t)^\beta \left(\frac{n}{\beta} + \lambda_t \right)^{n-1} - \beta(1 - \lambda_t)^{\beta-1} \left(\frac{n}{\beta} + \lambda_t \right)^n \right] \left[\Gamma_n \left(\frac{m}{\alpha} \right)^m + \langle \phi_n - \phi_t \rangle \right] \frac{1}{\lambda_t \delta_t}$$

Coupled Cohesive-Friction Model – Shear Decomposition

- Cohesive Forces

$$\mathbf{T} = \begin{Bmatrix} T_n \\ T_t \frac{\Delta_2}{\Delta_t} + T_F \left(\frac{|\Delta_2|}{\Delta_t} \right) \frac{\dot{\Delta}_2}{|\dot{\Delta}_2|} \\ T_t \frac{\Delta_3}{\Delta_t} + T_F \left(\frac{|\Delta_3|}{\Delta_t} \right) \frac{\dot{\Delta}_3}{|\dot{\Delta}_3|} \end{Bmatrix}$$

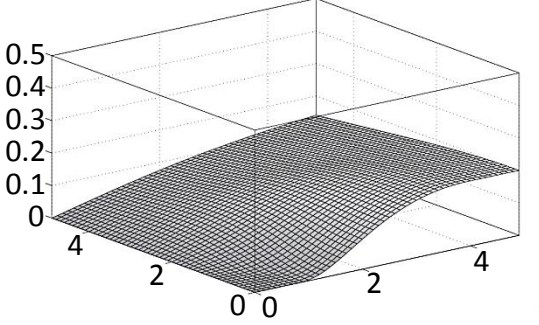
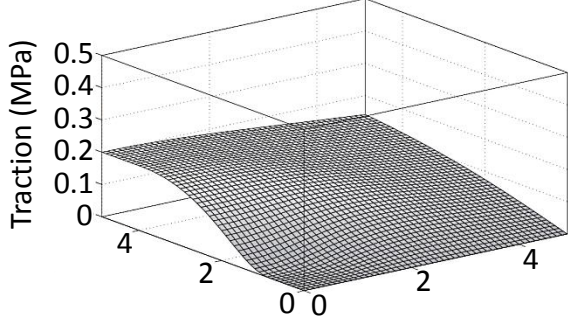


+

+

- Friction Forces

$$\mathbf{T} = \begin{Bmatrix} T_n \\ T_t \frac{\Delta_2}{\Delta_t} + T_F \left(\frac{|\Delta_2|}{\Delta_t} \right) \frac{\dot{\Delta}_2}{|\dot{\Delta}_2|} \\ T_t \frac{\Delta_3}{\Delta_t} + T_F \left(\frac{|\Delta_3|}{\Delta_t} \right) \frac{\dot{\Delta}_3}{|\dot{\Delta}_3|} \end{Bmatrix}$$

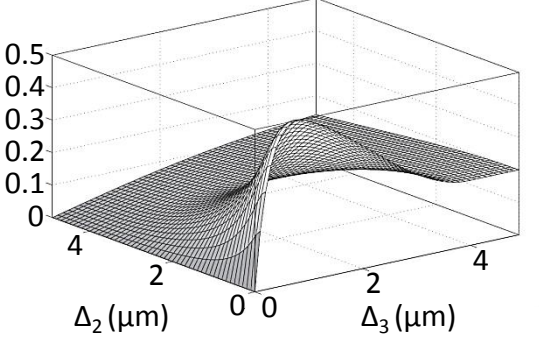
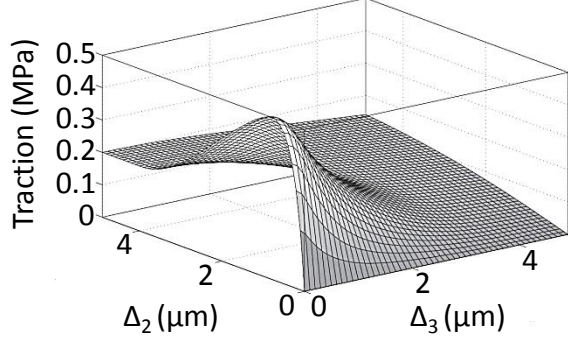


=

=

- Coupled Forces

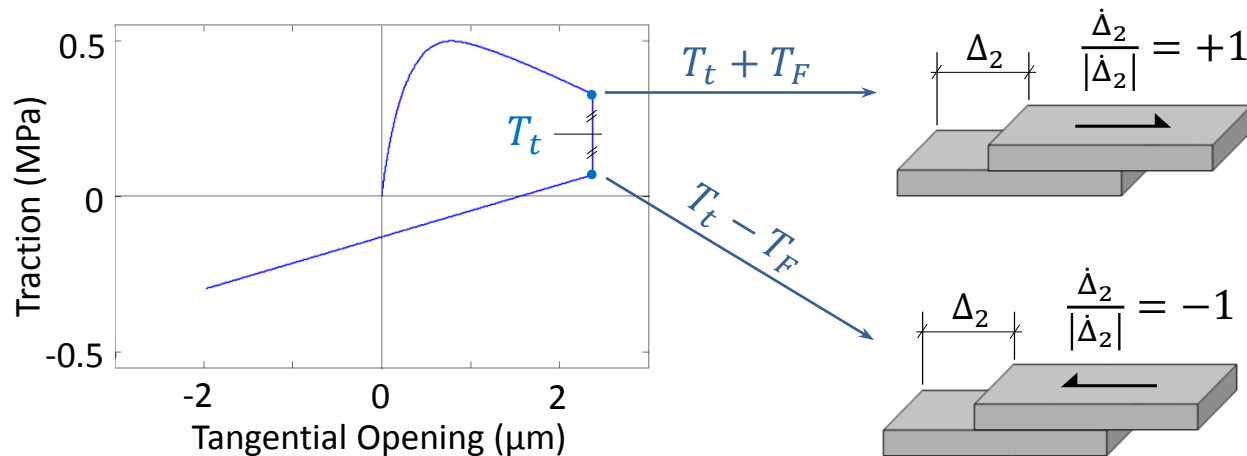
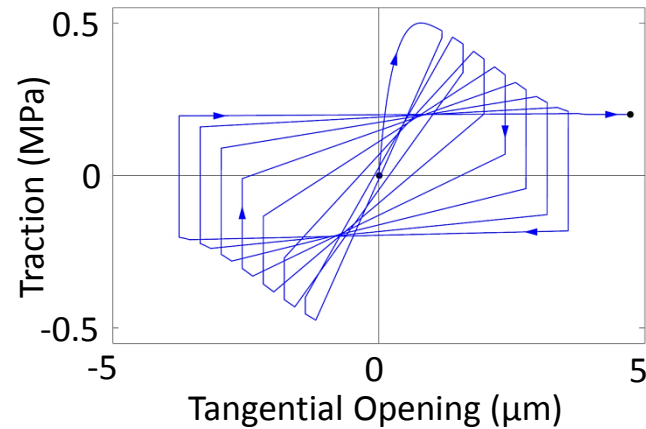
$$\mathbf{T} = \begin{Bmatrix} T_n \\ T_t \frac{\Delta_2}{\Delta_t} + T_F \left(\frac{|\Delta_2|}{\Delta_t} \right) \frac{\dot{\Delta}_2}{|\dot{\Delta}_2|} \\ T_t \frac{\Delta_3}{\Delta_t} + T_F \left(\frac{|\Delta_3|}{\Delta_t} \right) \frac{\dot{\Delta}_3}{|\dot{\Delta}_3|} \end{Bmatrix}$$



Coupled Cohesive-Friction Model

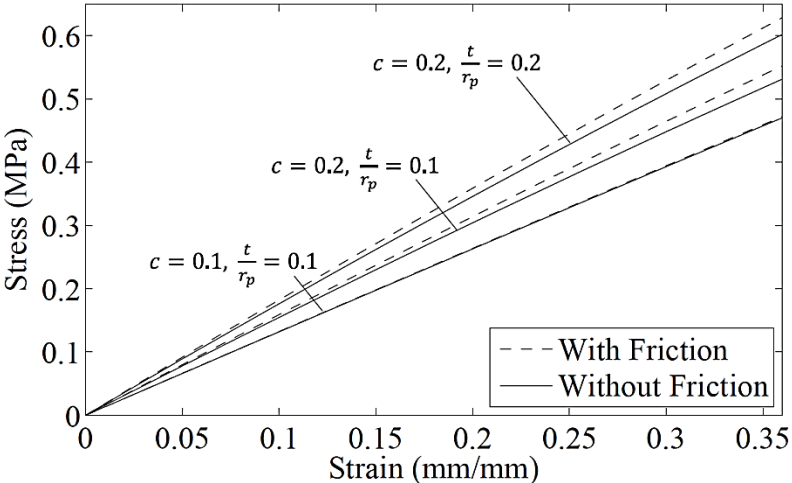
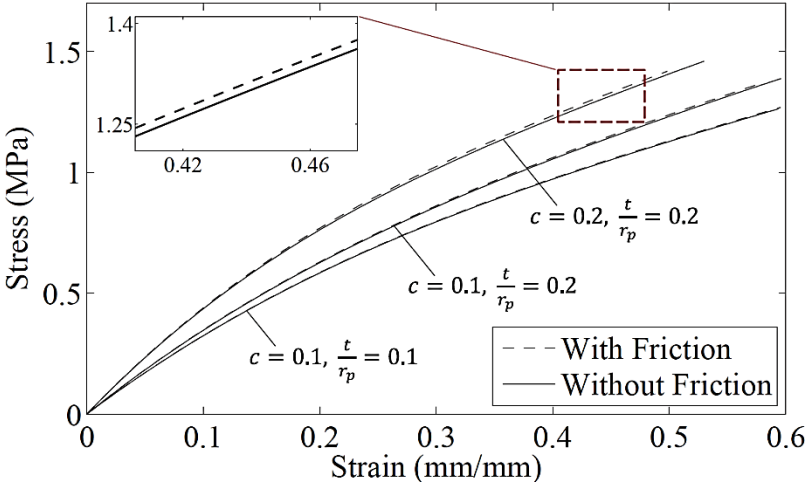
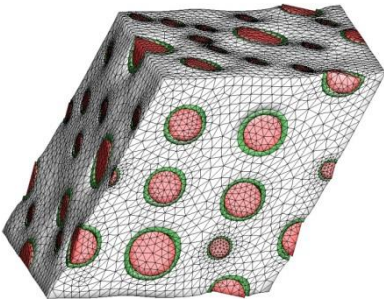
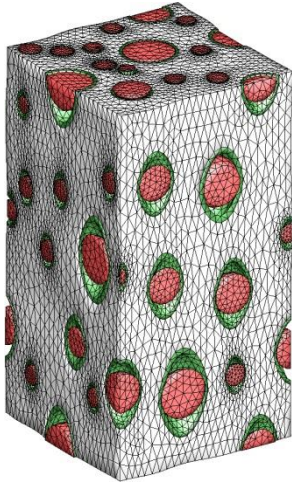
Frictional forces are not only separation dependent, but also direction dependent. This can most clearly be seen by observing the hysteretic response

$$\mathbf{T} = \begin{Bmatrix} T_t \frac{\Delta_2}{\Delta_t} + T_F \left(\frac{|\Delta_2|}{\Delta_t} \right) \frac{\dot{\Delta}_2}{|\dot{\Delta}_2|} \\ T_t \frac{\Delta_3}{\Delta_t} + T_F \left(\frac{|\Delta_3|}{\Delta_t} \right) \frac{\dot{\Delta}_3}{|\dot{\Delta}_3|} \end{Bmatrix}$$



Influence of Friction on Global Response

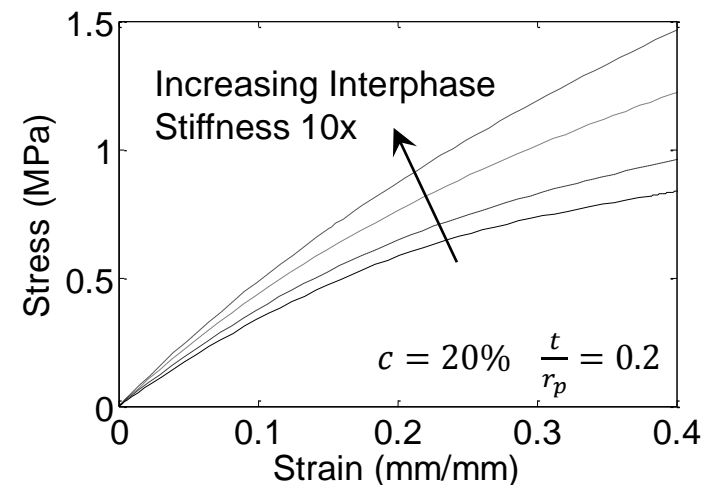
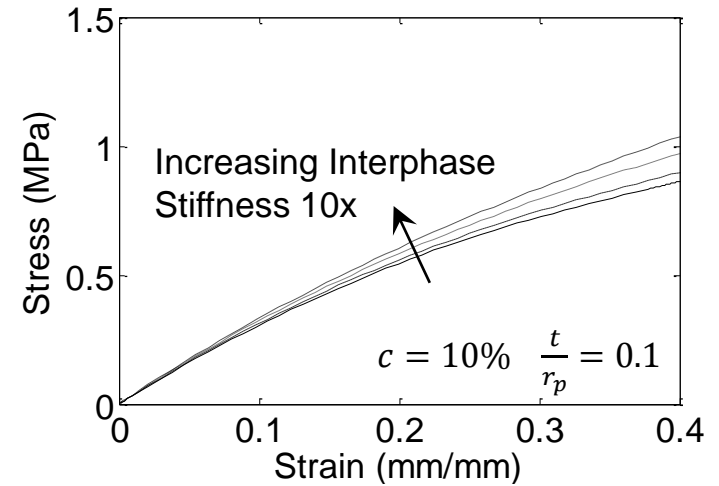
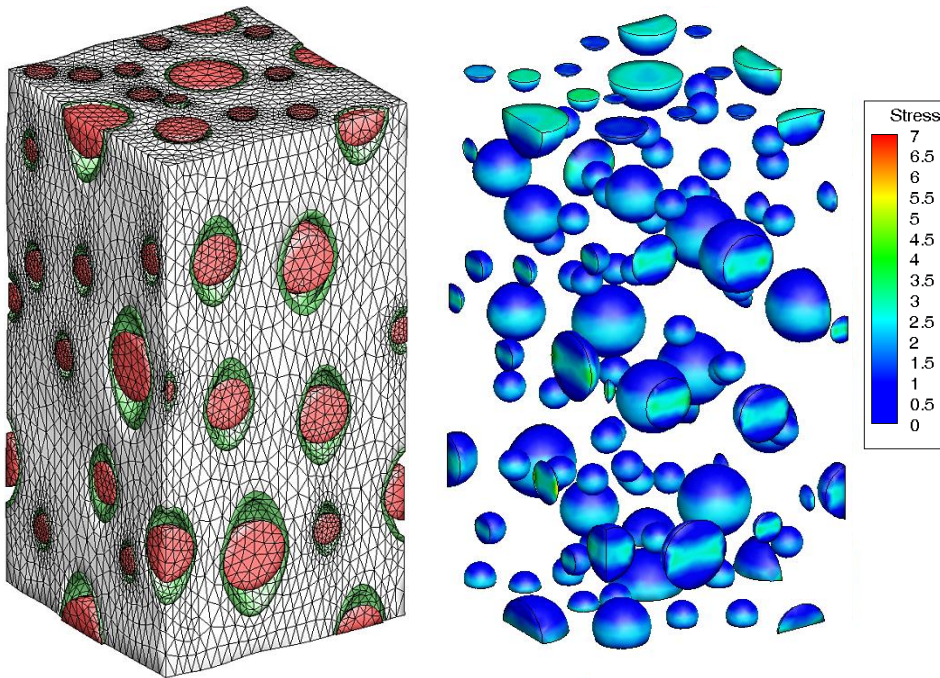
Frictional forces contribute little to the macroscopic constitutive response of the composite.



Spring, D. W. and Paulino, G.H., Computational homogenization of the debonding of particle reinforced elastomers: Considering interphases. *In Preparation*.

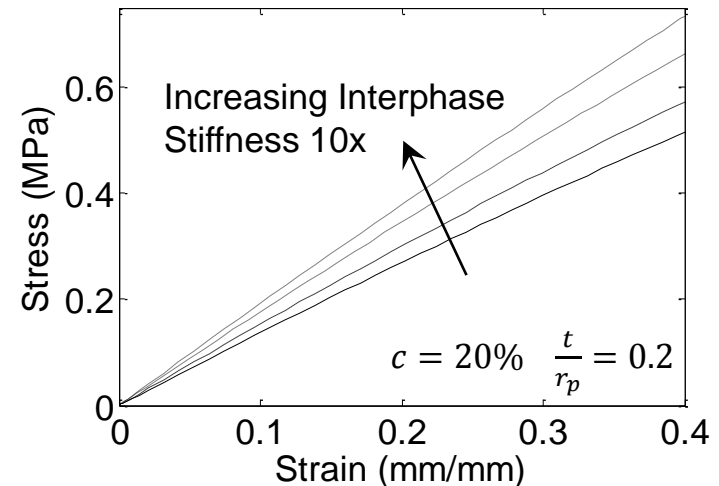
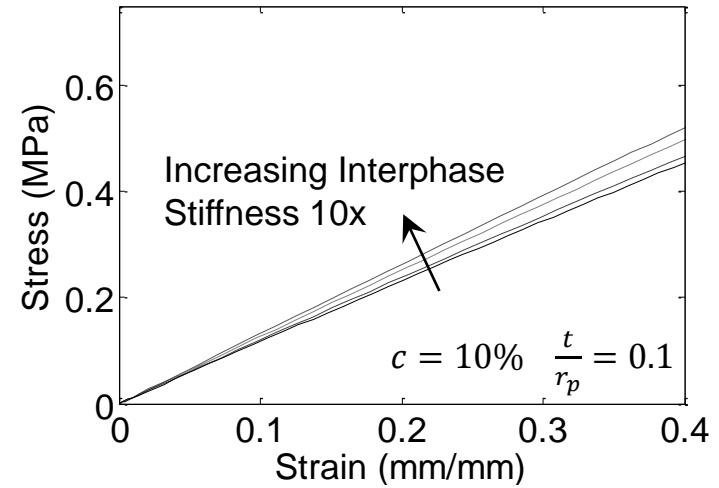
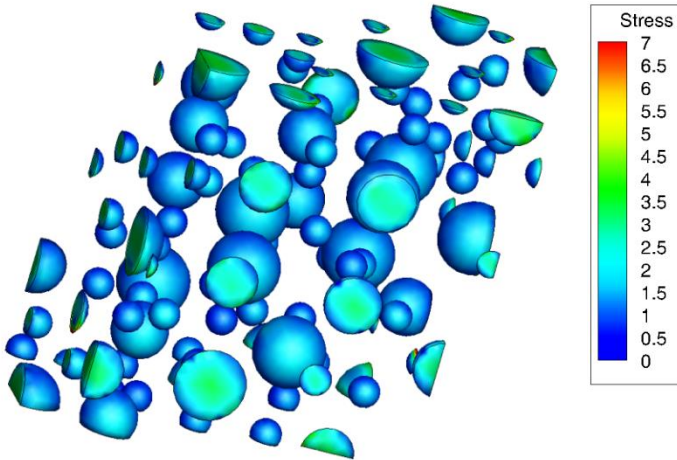
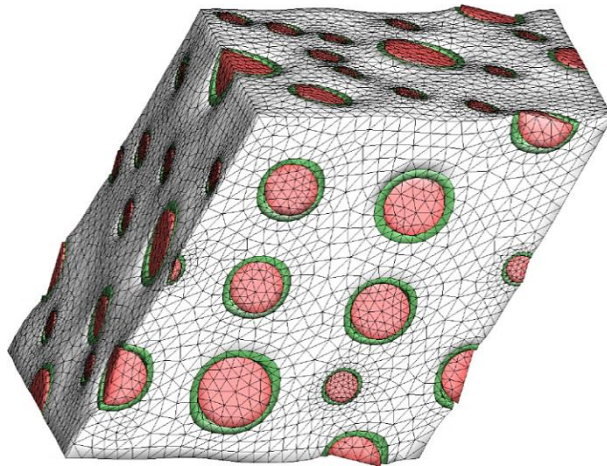
Results – Uniaxial Tension

The interphase stiffness and thickness (volume fraction) have varying effects on the global response under uniaxial tensions.



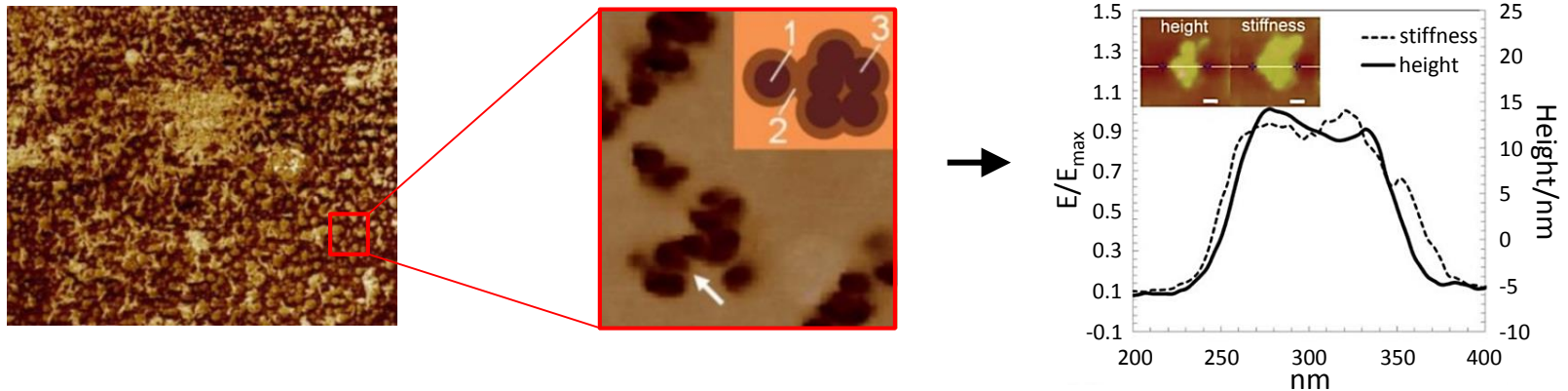
Results – Simple Shear

Similarly, in simple shear, the interphase stiffness and thickness (volume fraction) significantly influence the global response.



Concluding Remarks

- The presence of interphases and interfacial debonding significantly alters the macroscopic constitutive response of the composite material and should be considered when we model such composites.
- Interfacial debonding can be included through the use of cohesive elements.
- Frictional effects are negligible in tension induced debonding.
- The thickness (volume fraction) of the interphase has a greater effect on the behavior of the composite than the modulus.
- Recognizing the role and main factors influencing interfacial adhesion and proper surface modification may lead to significant progress in many fields of research and development, as well as related technologies.



Thank you for your attention!

Questions?

Daniel Spring
spring2@illinois.edu